Iraqi Journal of Science, 2025, Vol. 66, No. 11, pp: 5124- 5135
DOI: 10.24996/ijs.2025.66.11.34

ISSN: 0067-2904

An efficient mathematical model for the Outbreak of COVID-19 from the perspective of numerical analysis

Hossein Gholami[1], Mortaza Gachpazan[1]*, Majid Erfanian[2]*
[1]*Department of Applied Mathematics, Faculty of Mathematical Science, Ferdowsi University of Mashhad, Mashhad, Iran.*
[2]*Department of Mathematics, Faculty of Science, University of Zabol, Zabol, Iran*

Received: 21/9/2023 Accepted: 11/11/2024 Published: 30/11/2025

Abstract
In this paper, we developed an $S_M S_L EIRS_L$ epidemic model for COVID-19 by using compartmental analysis. In our model, we divided susceptible individuals into two separate groups: one for high-risk individuals and another for those at low risk. In this work, we have proved theorems about the non-negativity and boundedness of the solutions. Afterward, we obtained a disease-free equilibrium point and an endemic equilibrium point. We calculated the basic reproduction number using the next-generation matrix method and then we expressed theorems about the local and global stability of equilibria, finally, we have gone to the sensitivity analysis and numerical analysis.

Keywords: Susceptible individuals, High-risk individuals, Low-risk individuals, Basic reproduction number

1. Introduction

Infectious diseases, whether in the past, including smallpox, cholera, plague, tuberculosis, or in the contemporary era, including AIDS, influenza, Sars, Ebola, and now COVID-19 have challenged human societies and have always been one of the fundamental causes of death even in developed countries. Because a new infection may appear or previous infections may reappear and increase, the study of these diseases to predict and control them and their treatment is very important. Meanwhile, mathematical models can be used to study the behavior of the society involved in the disease and determine the policy that is used more effectively to deal with and eliminate the disease, these models are usually called epidemic models [1, 2]. In epidemic modeling, the studied population is based on the condition of the people about the progress of the disease they are divided into several subpopulations, transfers, and transitions between individuals of demographic groups, as well as any demographic changes such as birth, death, and migration are related to each other by mathematical equations, in this way, a dynamic system is obtained for the behavior of that population.

The mechanism of the spread of infectious diseases can be described by compartment models. For example, Kumar et al. in [3] proposed a new susceptible-exposed-infected-recovered-susceptible (SEIRS) dynamical model by including the vaccine rate. Asma et al. in

*Email: gachpazan@um.ac.ir

[4] studied a simple susceptible-vaccinated-infected-recovered (SVIR) type of model to investigate the coronavirus's dynamics in Saudi Arabia.
Researchers have used various systems of equations to model the COVID-19. Li and Guo [5] modeled a mutated form of this disease (Delta strain) with the help of ordinary differential equations and concluded that increasing the vaccination rate, isolation of infected persons and nucleic acid testing for all people will reduce the spread of this disease. Wang et al [6] divided the population into ten groups in their model and formed a non-linear differential equation system and evaluated the effect of quarantine and vaccination on the control of COVID-19. Torres et al. [7] modeled the disease of COVID-19 with the help of stochastic differential equations. To explain the behavior of the population, random perturbations of the white noise terms satisfying the Brownian motion have been governed by this system of equations. Hussain et al [8] presented stochastic differential equations. They obtained the related simulations, which help to realistic numerical data for the future prediction. Majid et al [9] presented the spatiotemporal dynamics of an epidemic spread using a compartmentalized PDE model. Their model was able to examine the effect of non-pharmaceutical intervention measures. Their model shows the efficacy of non-pharmaceutical interventions for mitigation. Babasola et al [10] considered a system of time-delay differential equations. The numerical results approved that the inclusion of delay destabilizes the system and makes the system show an oscillatory behavior which helps to obtain more insight into the transmission dynamics of the disease. Parsamanesh and erfanian [11] introduced a system of difference equations and studied types of bifurcations such as fold bifurcation, flip bifurcation and Neimark-Sacker bifurcation. In addition, interested readers can see the mathematical modeling of other infectious diseases such as dengue fever, Ebola, influenza, HIV/AIDS, typhoid fever, and monkeypox in [12-29] and the references therein.
In this article, the COVID-19 dynamics are divided into five distinct compartments: high-risk susceptible individuals (S_M), low-risk susceptible individuals(S_L), exposed individuals (E), infected individuals (I), and recovered individuals (R). The high-risk susceptible individuals (S_M) include those such as hospital staff, individuals with underlying conditions like asthma, or those who have not yet been vaccinated. In contrast, low-risk susceptible individuals (S_L) adhere to sanitary recommendations, wear face masks, do not have any underlying diseases, and have received at least one dose of the vaccine. The difference between S_M, S_L and E is that individuals in S_M and S_L groups have not yet been infected with the virus. While in E the group, there are individuals who have entered the body of the virus but still cannot transmit the virus to others.

This paper is organized as: The proposed model is presented in Section 2. The non-negativity and boundedness of the solutions have been proven in this section. In Section 3, the equilibrium points and basic reproduction number for the model are obtained. In Section 4, the stability of the model is expressed in the form of theorems and the local and global stability of the disease-free equilibrium point has been proven. Section 5 explores the sensitivity index and includes numerical analysis, while Section 6 presents the conclusion.

2. Model Development and Formulation

This revised model will consist of several compartments. At time t, the total human population, represented as $N(t)$, includes the dynamics of low-risk susceptible individuals (S_L), high-risk susceptible individuals (S_M), exposed individuals (E), and infected individuals (I), and the compartment of recovered individuals (R). If we denote the total population by N, then we have

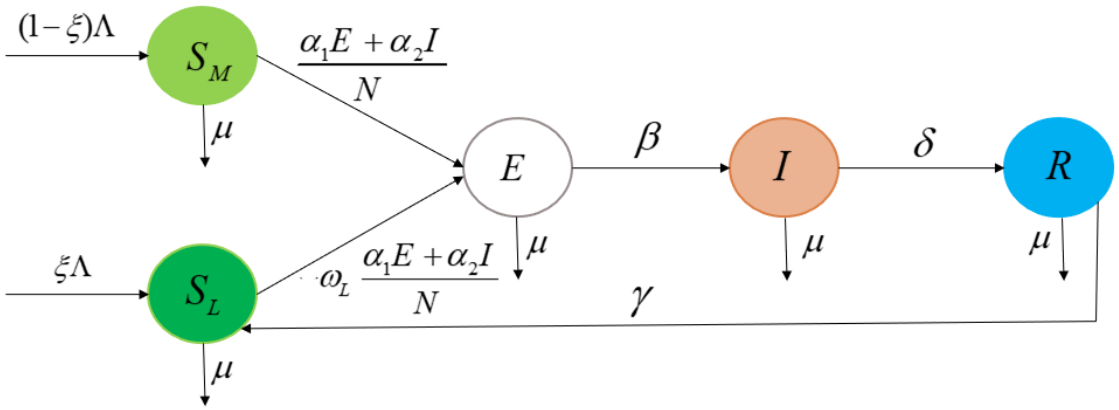

Figure 1: The schematic model flow.

$$N(t) = S_M(t) + S_L(t) + E(t) + I(t) + R(t). \quad (1)$$

The model parameters are introduced in Table 1.

Table 1: Description of the model parameters.

Parameters	Description
Λ	Rate of recruitment (from birth and immigration).
μ	Rate of natural mortality and rate of mortality due to disease.
α_1	The transition rate of infection from E class.
α_2	The transition rate of infection from I class.
ξ	The proportion of individuals entered the population with low-risk susceptibility to the disease.
ω_L	Reduction of the risk factor of infection in the compartment S_L.
β	Exit rate from the E compartment.
δ	The recovery rate of infected individuals.
γ	Rate at which temporary immunity wanes following recovery.

The model is formulated mathematically through a set of ordinary differential equations:

$$\begin{aligned}
\frac{dS_M}{dt} &= (1-\xi)\Lambda - \frac{\alpha_1 E+\alpha_2 I}{N} S_M - \mu S_M,\\
\frac{dS_M}{dt} &= \xi\Lambda + \gamma R - \omega_L \frac{\alpha_1 E+\alpha_2 I}{N} S_L - \mu S_L,\\
\frac{dE}{dt} &= (S_M + \omega_L S_L)\left(\frac{\alpha_1 E+\alpha_2 I}{N}\right) - \beta E - \mu E,\\
\frac{dI}{dt} &= \beta E - \delta I - \mu I,\\
\frac{dR}{dt} &= \delta I - \gamma R - \mu R.
\end{aligned} \quad (2)$$

From summing the equations of model (2), we can conclude that

$$\frac{dN}{dt} = \Lambda - \mu N. \quad (3)$$

The region described below encompasses the dynamics of the model:

$$\Omega = \{(S_M, S_L, E, I, R) \in R_+^5 : N \leq \frac{\Lambda}{\mu}\}. \quad (4)$$

Theorem 2.1. The initial conditions for the model's variables are specified as follows $\{S_M(0) \geq 0, S_L(0) \geq 0, E(0) \geq 0, I(0) \geq 0, R(0) \geq 0 \text{ and } N(0) \geq 0\} \in \Omega$, then the solution set $\{S_M(t), S_L(t), E(t), I(t), R(t) \text{ and } N(t)\}$ is non-negative Ω for all time $t \geq 0$.

Proof. To demonstrate that the variables S_L and S_M remain positive for all $t \geq 0$, we employ a proof by contradiction. We begin by assuming that a trajectory intersects one of the positive cones at times t_1 or t_2 such that:

$$t_1 : S_L(t_1) = 0, \frac{dS_L}{dt}(t_1) < 0, S_M(t) > 0, E(t) > 0, I(t) > 0 \text{ and } R(t) > 0 \text{ for } t \in (0, t_1), \text{or}$$

$$t_2 : S_M(t_2) = 0, \frac{dS_M}{dt}(t_2) < 0, S_L(t) > 0, E(t) > 0, I(t) > 0 \text{ and } R(t) > 0 \text{ for } t \in (0, t_2).$$

By utilizing the second equation from system (2), we derive from the first assumption:

$$\frac{dS_L}{dt}(t_1) = \xi\Lambda + \gamma R > 0,$$

which contradicts the first assumption that $\frac{dS_L}{dt}(t_1) < 0$.

Therefore, we conclude that $S_L(t)$ remains positive for all $t \geq 0$. Let t_1 be chosen so that the corresponding point is on the positive axis of $S_L(t)$, which implies $R(t_1) > 0$.

Now, employing the first equation from system (2), we get:

$$\frac{dS_M}{dt}(t_2) = (1 - \xi)\Lambda > 0,$$

also contradicts the assumption $\frac{dS_M}{dt}(t_2) < 0$. Hence, $S_M(t)$ remains positive for all $t \geq 0$.

Assuming $\lambda = \frac{\alpha_1 E + \alpha_2 I}{N}$ and According to the third equation of system (2), we can determine that:

$$\frac{dE}{dt} = (S_M + \omega_L S_L)\lambda - (\beta + \mu)E \geq -(\beta + \mu), \quad (5)$$

Since $S_M(t)$ and $S_L(t)$ are non-negative for $t \geq 0$. Solving Equation (5) results,

$E(t) \geq E(0)\, exp(-(\beta + \mu)t) \geq 0.$

Likewise, from the fourth equation of (2), we get,

$$\frac{dI}{dt} = \beta E - (\delta + \mu)I \geq -(\delta + \mu)I. \quad (6)$$

Solving (6) yields,

$$I(t) \geq I(0)\, exp(-(\delta + \mu)t). \quad (7)$$

Finally, using the last equation of system (2), we have,

$$\frac{dR}{dt} = \delta I - (\gamma + \mu)R \geq -(\gamma + \mu)R. \quad (8)$$

Solving (8) leads to,

$R(t) \geq R(0)\, exp(-(\gamma + \mu)t) \geq 0.$

Thus, any solution of system (2) is non-negative for $t \geq 0$ and any initial condition in Ω. ■

Theorem 2.2. All solutions of the model (2) are bounded.

Proof. As previously discussed, we have the differential equation $\frac{dN}{dt} = \Lambda - \mu N$.

By separating variables and proceeding with integration, we have:

$$\int \frac{dN}{\Lambda - \mu N} = \int dt,$$
$$\Rightarrow -\frac{1}{\mu} ln(\Lambda - \mu N) = t + c,$$
$$\Rightarrow ln(\Lambda - \mu N) = -\mu t + C, \quad \text{where } C = -\mu c$$
$$\Rightarrow Log_e^{(\Lambda - \mu N)} = -\mu t + C,$$
$$\Rightarrow \Lambda - \mu N = exp(-\mu t + C),$$
$$\Lambda - \mu N = A\, exp(-\mu t), \tag{9}$$

where in Equation (9), $A = exp(-\mu C)$.
It can be written from the (9) that

$$\mathrm{N(t)} = \frac{1}{\mu}(\Lambda - \mathrm{A}\exp(-\mu \mathrm{t})). \tag{10}$$

To determine the initial population size N_0 we substitute $t = 0$ into the last equality. So,

$$N(0) = \frac{\Lambda}{\mu} - \frac{A}{\mu} = \frac{\Lambda - A}{\mu} = N_0, \tag{11}$$
$$\Rightarrow A = \Lambda - \mu N_0. \tag{12}$$

By replacing (12) with (11), we get

$$N(t) = \frac{\Lambda}{\mu} - \left(\frac{\Lambda - \mu N_0}{\mu}\right) exp(-\mu t). \tag{13}$$

From (13), as t approaches infinity, $N(t)$ converges to $\frac{\Lambda}{\mu}$. Therefore, the positive solutions of model (2) are bounded.

■

3. Mathematical examination of the model

To find the equilibrium points, we set the right-hand side of model (2) to zero, resulting in:

$$\begin{aligned}
(1-\xi)\Lambda - \frac{\alpha_1 E + \alpha_2 I}{N} S_M - \mu S_M &= 0,\\
\xi\Lambda + \gamma R - \omega_L \frac{\alpha_1 E + \alpha_2 I}{N} S_L - \mu S_L &= 0,\\
(S_M + \omega_L S_L)\left(\frac{\alpha_1 E + \alpha_2 I}{N}\right) - \beta E - \mu E &= 0,\\
\beta E - \delta I - \mu I &= 0,\\
\delta I - \gamma R - \mu R &= 0.
\end{aligned} \tag{14}$$

Our model features both disease-free and endemic equilibria, which can be identified using (14). We denote the disease-free equilibrium point $DFEP$ as

$$X_{dfep} = \left(S_{M\,dfep}, S_{L\,dfep}, E_{dfep}, I_{dfep}, R_{dfep}\right) = (1-\xi, \xi, 0, 0, 0).$$

Additionally, the endemic equilibrium point (EEP) is designated as

$$X_{eep} = \left(S_{M\,eep}, S_{L\,eep}, E_{eep}, I_{eep}, R_{eep}\right).$$

where,

$$\begin{aligned}
S_{M\,eep} &= \frac{(1-\xi)\Lambda}{\lambda_0^\star + \mu},\\
S_{L\,eep} &= \frac{\xi\Lambda + \gamma R}{\mu + \omega_L \lambda_0^\star},\\
E_{eep} &= \frac{(S_M + \omega_L S_L)\lambda_0^\star}{\beta + \mu},\\
I_{eep} &= \frac{\beta E}{\delta + \mu},\\
R_{eep} &= \frac{\delta I}{\gamma + \mu}.
\end{aligned} \tag{15}$$

Also, $\lambda_0^\star = \frac{\alpha_1 E + \alpha_2 I}{N}$.

The basic reproduction number of the model is represented by $\mathcal{R}_0$ which determines whether the infection spreads throughout the population. To achieve this, we utilize the next-generation matrix method [30]. The compartments that directly contribute to the spread of COVID-19 are represented by the second, third, and fourth equations of model (2). These equations can be written as

$$\frac{dz}{dt} = \Phi(z) - \Psi(z),$$

where

$$z = (E, I)^T, \Phi(z) = \begin{bmatrix} (S_M + \omega_L S_L)\left(\frac{\alpha_1 E + \alpha_2 I}{N}\right) \\ 0 \end{bmatrix} \text{and } \Psi(z) = \begin{bmatrix} (\mu + \beta)E \\ -\beta E + (\delta + \mu)I \end{bmatrix}.$$

Where G and H are the Jacobian matrices of Φ and Ψ evaluated at the $DFEP\left(X_{dfep}\right)$, respectively. The entries of the first column of these matrices are derived by differentiating the respective entries of the matrices $\Phi(z)$ and $\Psi(z)$ with respect to the variables E and I at the $DFEP$. Specifically, they are given by,

$$G = \frac{\partial \Phi(X_{dfep})}{\partial x_j} = \begin{bmatrix} \frac{\alpha_1}{N}(1 - \xi + \omega_L \xi) & \frac{\alpha_2}{N}(1 - \xi + \omega_L \xi) \\ 0 & 0 \end{bmatrix}$$

and

$$H = \frac{\partial \Psi(X_{dfep})}{\partial x_j} = \begin{bmatrix} (\mu + \beta) & 0 \\ -(\beta) & (\delta + \mu) \end{bmatrix}, \tag{16}$$

where $x_j = E, I$.

The $\mathcal{R}_0$ is the largest eigenvalue (the spectral radius) of the matrix GH^{-1}, therefore,

$$\mathcal{R}_0 = \frac{1}{N}(1 - \xi + \omega_L \xi)\frac{1}{\beta + \mu}\left(\alpha_1 + \frac{\alpha_2 \beta}{\delta + \mu}\right). \tag{17}$$

4. Stability analysis

In this section, we have demonstrated the local asymptotic stability and global asymptomatic stability of the disease-free equilibrium point in the form of two theorems.

Theorem 4.1. The disease-free equilibrium point (X_{dfep}) is locally asymptotically stable if:

(i) $\beta + \delta + 2\mu > (1 - \xi + \omega_L \xi)\frac{\alpha_1}{N}$,

(ii) $\mathcal{R}_0 < 1$.

Proof. The Jacobian matrix of (2) at the $DFEP\left(X_{dfep}\right)$ is given by,

$$J\left(X_{dfep}\right) = \begin{bmatrix} -(\mu) & 0 & -\frac{\alpha_1}{N}(1 - \xi) & -\frac{\alpha_2}{N}(1 - \xi) & 0 \\ 0 & -(\mu) & -(\omega_L \xi)\frac{\alpha_1}{N} & -(\omega_L \xi)\frac{\alpha_2}{N} & (\gamma) \\ 0 & 0 & (1 - \xi + \omega_L \xi)\frac{\alpha_1}{N} - (\beta + \mu) & (1 - \xi + \omega_L \xi)\frac{\alpha_2}{N} & 0 \\ 0 & 0 & (\beta) & -(\delta + \mu) & 0 \\ 0 & 0 & 0 & (\delta) & -(\gamma + \mu) \end{bmatrix}.$$

The eigenvalues of $J\left(X_{dfep}\right)$ are $-\mu$ (with multiplicity of 2), $-(\gamma + \mu)$ and the roots of the second-degree polynomial that is given by,

$$D_0\lambda^2 + D_1\lambda + D_2 = 0,$$

Where

$$D_0 = 1,$$
$$D_1 = \beta + \delta + 2\mu - (1 - \xi + \omega_L\xi)\frac{\alpha_1}{N},$$
$$D_2 = (\beta + \mu)(\delta + \mu)[1 - \mathcal{R}_0].$$

Based on Routh-Hurwitz criteria, a sufficient condition for the roots of polynomial $D_0\lambda^2 + D_1\lambda + D_2$ to be negative or have a negative real part is that $D_1, D_2 > 0$.
Using the assumptions of the theorem, it is easy to see that $D_1 > 0$. Additionally, the condition $D_2 > 0$ is equivalent to the condition $\mathcal{R}_0 < 1$.

■

Theorem 4.2. The $DFEP$ of the model (2) is globally asymptotically stable if $\mathcal{R}_0 < 1$.

Proof. Let us consider a Lyapunov function V_{dfep} defined by

$$V_{dfep} = B_1E + B_2I, \tag{18}$$

where

$$B_1 = \delta + \mu,$$
$$B_2 = \frac{\alpha_2}{N}(1 - \xi + \omega_L\xi). \tag{19}$$

The time derivation of Function (18) is,

$$\frac{dV_{dfep}}{dt} = B_1\frac{dE}{dt} + B_2\frac{dI}{dt}. \tag{20}$$

By substituting the corresponding values from model (2) instead of $\frac{dE}{dt}$ and $\frac{dI}{dt}$ at the $DFEP$ then we have,

$$\begin{aligned}\frac{dV_{dfep}}{dt} &= B_1[(1 - \xi + \omega_L\xi)\left(\frac{\alpha_1E + \alpha_2I}{N}\right) - (\beta + \mu)E] + B_2[\beta E - (\delta + \mu)I] \\ &= (\delta + \mu)[(1 - \xi + \omega_L\xi)\left(\frac{\alpha_1E + \alpha_2I}{N}\right) - (\beta + \mu)E] \\ &\quad + \frac{\alpha_2}{N}(1 - \xi + \omega_L\xi)[\beta E - (\delta + \mu)I].\end{aligned} \tag{21}$$

The expansion of Equation (21) yields,

$$\begin{aligned}\frac{dV_{dfep}}{dt} &= \frac{\alpha_1}{N}(\delta + \mu)(1 - \xi + \omega_L\xi)E \\ &\quad + \frac{\alpha_2}{N}(\delta + \mu)(1 - \xi + \omega_L\xi)I \\ &\quad -(\delta + \mu)(\beta + \mu)E \\ &\quad + \frac{\alpha_2}{N}(1 - \xi + \omega_L\xi)\beta E \\ &\quad -\frac{\alpha_2}{N}(\delta + \mu)(1 - \xi + \omega_L\xi)I.\end{aligned} \tag{22}$$

The sum of the second term and fifth term on the right-hand side of Equation (22) is equal to zero. Thus

$$\frac{dV_{dfep}}{dt} = (\delta+\mu)(\beta+\mu)E \times [\frac{\alpha_1}{N}\frac{1}{\beta+\mu}(1-\xi+\omega_L\xi) + \frac{\alpha_2}{N}\frac{\beta}{(\delta+\mu)(\beta+\mu)}(1-\xi+\omega_L\xi) - 1] = (\delta+\mu)(\beta+\mu)[\mathcal{R}_0 - 1]E \quad (23)$$

Since all parameters are assumed to be positive and according to Theorem 2.1, variable E is positive, therefore $\frac{dV_{dfep}}{dt} \leq 0$, if $\mathcal{R}_0 < 1$. It finishes the proof of Theorem 4.2.■

5. Sensitivity index and numerical experiments

To determine how sensitive a model is to changes in parameters, sensitivity analysis is employed. The normalized forward sensitivity index of the basic reproduction number $\mathcal{R}_0$ which differentially depends on a parameter ρ, is defined as: $\Upsilon_{\rho}^{\mathcal{R}_0} = \frac{\partial \mathcal{R}_0}{\partial \rho} \times \frac{\rho}{\mathcal{R}_0}$.

We repeated the above formula for all the variables that $\mathcal{R}_0$ depended on got the result $\Upsilon_p^{\mathcal{R}_0} > 0$ for $p = \omega_L, \alpha_1, \alpha_2$ and β. In other words, $\mathcal{R}_0$ has a direct relationship with these parameters and $\mathcal{R}_0$ increases with increasing parameters and vice-versa. Also, $\Upsilon_q^{\mathcal{R}_0} < 0$ for $q = \xi, \mu$ and δ. In other expression, $\mathcal{R}_0$ increases (decreases) with decrease (increase) of these parameters. Numerical results for our model were performed using the parameter values in Table 2. All parameters are assumed. Simulation for the model (2) is conducted using MATLAB $R2016b$

Table 2: Model parameter values

Parameter	value
Λ	0.029
β	0.018
α_1	0.5
α_2	0.036
ξ	0.296
δ	0.8
ω_L	0.4
γ	0.17
μ	0.000036

encoded with a $ODE45$ solver, with an initial population of $S_M(0) = 23$, $S_L(0) = 40, E(0) = 19$, $I(0) = 38$ and $R(0) = 45$.

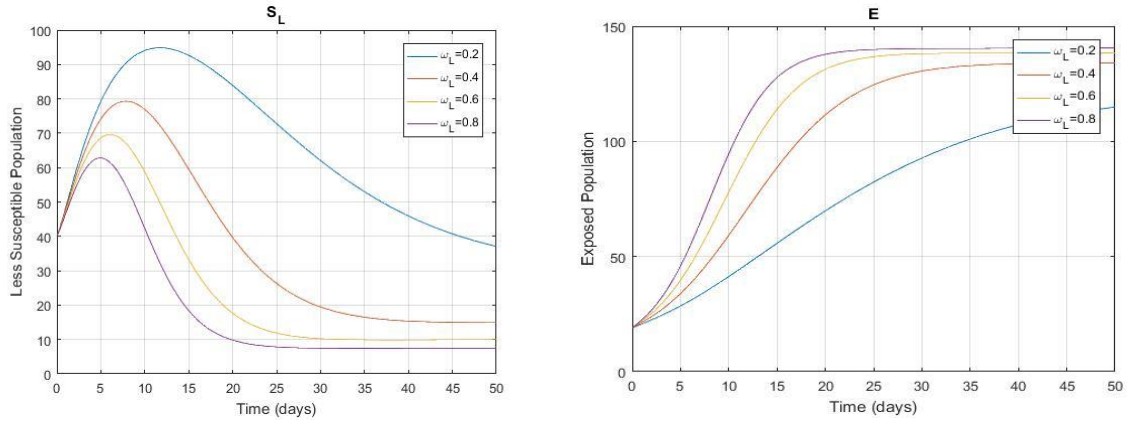

Figure 2: Solution curves depicting the impact of reduction of the risk factor of infection in the S_L compartment (ω_L) on S_L and E classes of the model (2).

It can be seen from Figure 2, as reduction of the risk factor of infection in the low-risk susceptible individuals (ω_L) increases, $\omega_L \frac{\alpha_1 E+\alpha_2 I}{N}$ fraction increases. As a result, the population of low-risk susceptible individuals (S_L) decreases and the population of exposed individuals (E) increases.

From Figure 3, we can realize that increasing the recovery rate of infected individuals (δ) is not sufficient to increase the population of recovered individuals (R). After the passage of time and due to the weakening of the immune system, a significant number of recovered individuals (R) are joined to the low-risk susceptible individuals (S_L) compartment. This decrease in the population of R class is the result of this issue.

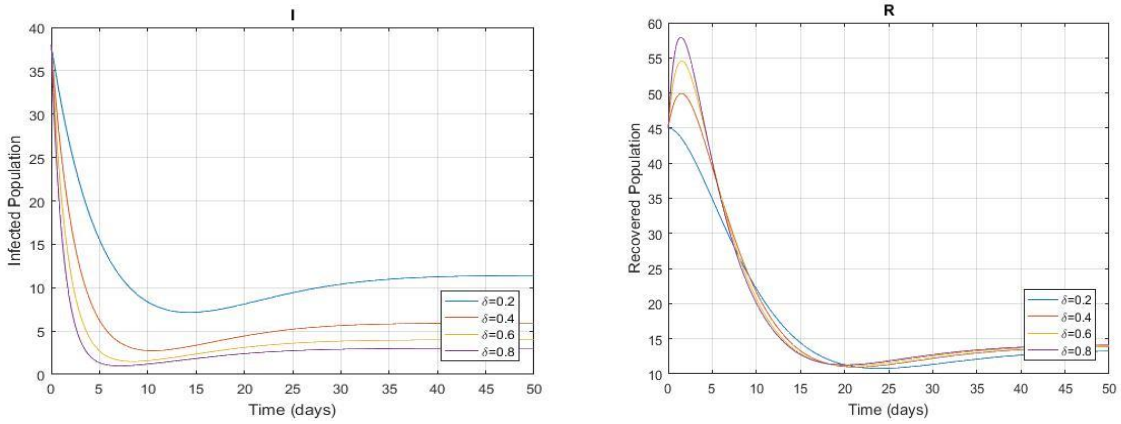

Figure 3: Solution curves depicting the impact of the recovery rate of infected individuals (δ) on I and R compartments of the model (2).

Figure 4 shows that as the rate of reduction of the temporary immunity effect increases, the population of high-risk susceptible individuals (S_M) goes to zero with a very steep slope. The reason is that people who have been infected once are placed in S_L compartment. Population of S_L class initially increases and then decreases and finally becomes uniform. The population of the group E also increases significantly and the population of the I group decreases rapidly and converge to a certain point. Finally, the population of the group R decreases with the increase of γ.

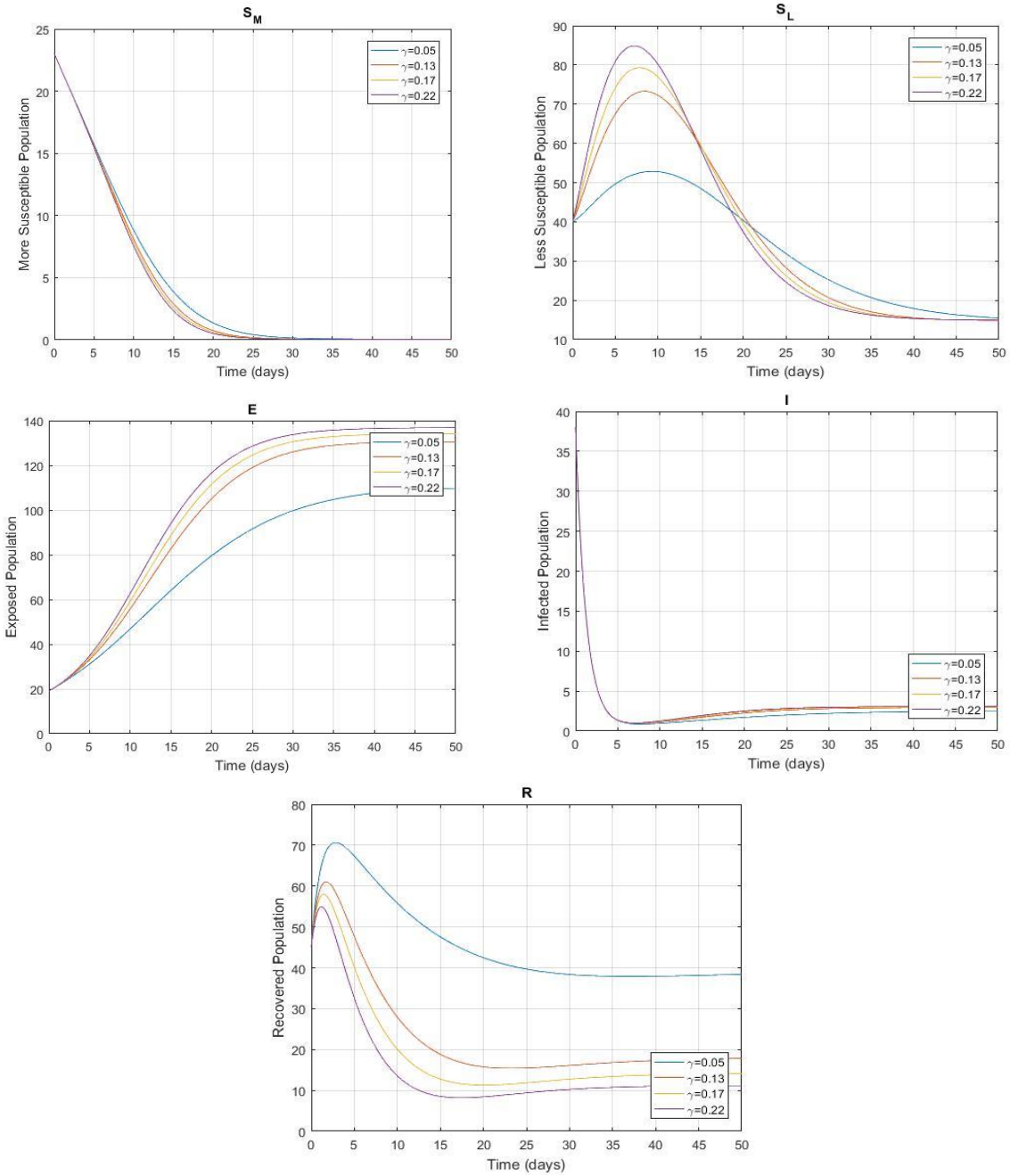

Figure 4: Solution curves depicting the impact of rate of reduction of the effect of temporary immunity after the recovery (γ) on all of the compartments of the model (2).

6. Conclusions

In this paper, we categorized susceptible individuals into two distinct compartments: high-risk susceptible individuals and low-risk susceptible individuals. We demonstrated that the solutions of our model are non-negative and bounded. We computed the basic reproduction number using the next-generation matrix method. We obtained the disease-free and endemic equilibria. We proved the disease-free equilibrium is locally and globally stable using the Jacobian and Lyapunov function methods, respectively. Additionally, we used the reduction risk factor of infection in the low-risk susceptible individuals compartment (S_L). We applied sensitivity analysis to find out, which parameters have a direct or inverse relationship with the basic reproduction number. Numerical results displayed that with the increase of ω_L, the number of low-risk susceptible individuals (S_L) decreases and the population of exposed

individuals (E) increases. In addition, the recovery rate of infected individuals (δ) is not an influential parameter for increasing the population of recovered individuals (R).

References

[1] F. Brauer and C. C. Chavez, "Mathematical models in population biology and epidemiology," *Springer,* 2012.

[2] O. Diekmann and J. A. P. Heesterbeek, "Mathematical epidemiology of infectious diseases: model building, analysis and interpretation," *John Wiley and Sons, International Journal of Epidemiology*, vol. 30*,* pp. 186*,* 2000.

[3] P. Kumar, V. Erturk, and M. M. Arcila, "A new fractional mathematical modelling of COVID-19 with the availability of vaccine," *Results in Physics,* vol. 24, pp. 104213, 2021.

[4] Asma, M. Yousaf, M. Afzaal, M. H. DarAssi, M. A. Khan, M. Y. Alshahrani, and M. Suliman, "A mathematical model of vaccinations using new fractional order derivative," *Vaccines*, vol. 10, pp. 1980, 2022.

[5] T. Li and Y. Guo, "Modeling and optimal control of mutated COVID-19 (Delta strain) with imperfect vaccination," *Chaos, Solitons and Fractals, Nonlinear Science,and Nonequilibrium and Complex Phenomena,* vol. 156, p. 111825, 2022.

[6] F. Wang, L. Cao, and X. Song, "Mathematical modeling of mutated COVID-19 transmission with quarantine, isolation and vaccination," *Mathematical Biosciences and Engineering*, vol.19, no. 8, pp. 8035-8056, 2022.

[7] D. N. Torres, A. R. Gutierrez, V. Arunachalam, C. Ohajunwa, and P. Seshaiyer, "Stochastic modeling, analysis, and simulation of the COVID-19 pandemic with explicit behavioral changes in Bogota: A case study," *Infectious Disease Modelling,* vol. 7, pp. 199-211, 2022.

[8] S. Hussain, E. N. Madi, H. Khan, S. Etemad, S. Rezapour, T. Sitthiwirattham, and N. Patanarapeelert, "Investigation of the stochastic modeling of COVID-19 with environmental noise from the analytical and numerical point of view," *Mathematics,* vol. 9,pp. 3122, 2021.

[9] F. Majid, A. M. Deshpande, S. Ramakrishnan, S. Ehrlich, and M. Kumar, "Analysis of epidemic spread dynamics using a PDE model and COVID-19 data from Hamilton County OH USA," *IFAC PapersOnLine,* vol. 54, pp. 322-327, 2021.

[10] O. Babasola, O. Kayode, O. J. Peter, F. C. Onwuegbuche, and F. A. Oguntolu, "Time delayed modelling of the COVID-19 dynamics with a convex incidence rate," *Informaticsin Medicine Unlocked,* vol. 35, pp. 101124, 2022.

[11] M. Parsamanesh and M. Erfanian, "Stability and bifurcations in a discrete-time SIVSmodel with saturated incidence rate," *Chaos, Solitons and Fractals, Nonlinear Science,and Nonequilibrium and Complex Phenomena,* vol. 150, pp. 111178, 2021.

[12] M. Aguiar, V. Anam, K. B. Blyuss, C. D. S. Estadilla, B. V. Guerrero, D. Knopoff, B. W. Kooi, A. K. Srivastav, V. Steindorf, and N. Stollenwerk, "Mathematical models for dengue fever epidemiology: A 10- year systematic review," *Physics of Life Reviews,* vol. 40, pp. 65-92, 2022.

[13] S. T. Ogunlade, M. T. Meehan, A. I. Adekunle, and E.S. McBryde, "A systematic review of mathematical models of dengue transmission and vector control: 2010-2020," *viruses,* vol. 15, pp. 254, 2023.

[14] A. Din, T. Khan, Y. Li, H. Tahir, A. Khan, and W. A. Khan, "Mathematical analysis of dengue stochastic epidemic model," *Results in Physics,* vol. 20, pp. 103719, 2021.

[15] S. D. D. Njankou and F. Nyabadza, "Modelling the role of human behavior in Ebola virus disease (EVD) transmission dynamics," *Computational and Mathematical Methods in Medicine,* vol. 2022, pp. 11, 2022.

[16] R. T. Abah, A. B. Zhiri, K. Oshinubi, and A. Adeniji, "Mathematical analysis and simulation of Ebola virus disease spread incorporating mitigation measures," *Franklin Open,* vol. 6, pp. 100066, 2024.

[17] A. Rachah, "A mathematical model with isolation for the dynamics of Ebola virus,"*IOP Conf. Series: Journal of Physics,* vol. 1132, no.1, pp. 012058, 2018.

[18] C. A. Beauchemin and A. Handel, "A review of mathematical models of influenza Ainfections within a host or cell culture: lessons learned and challenges ahead," *BMC Public Health,* vol. 11, pp. 1- 15, 2011.

[19] C. W. Kanyiri, K. Mark, and L. Luboobi, "Mathematical analysis of Influenza A dynamics in the emergence of drug resistance," *Computational and Mathematical Methods in Medicine*, vol. 2018, no.1, pp. 2434560, 2018.

[20] F. Evirgen, E. Ucar, S. Ucar, and N. Ozdemir, "Modelling influenza a disease dynamics under Caputo-Fabrizio fractional derivative with distinct contact rates," *Mathematical Modelling and Numerical Simulation with Applications,* vol. 3, pp. 58-73, 2023.

[21] R. Arias, K. D. Angeles, S. Maleki, and R. R. Ahangar, "Mathematical modeling of the HIV-AIDS epidemic," *Open Access Library Journal*, vol. 9, pp. e7972, 2022.

[22] T. K. Ayele, E. F. D. Goufo, and S. Mugisha, "Mathematical modeling of HIV/AIDS with optimal control: A case study in Ethiopia," *Results in Physics*, vol. 26, pp. 104263, 2021.

[23] Attaullah and M. Sohaib, "Mathematical modeling and numerical simulation of HIV infection model," *Results in Applied Mathematics,* vol. 7, pp. 100118, 2020.

[24] A. K. Suhuyini and B. Seidu, "A mathematical model on the transmission dynamics of typhoid fever with treatment and booster vaccination," *Frontiers in Applied Mathematics and Statistics,* vol. 9*,* pp. 1151270, 2023.

[25] I. U. Khan, S. Mustafa, A. Shokri, S. Li, A. Akgul, and A. Bariq, "The stability analysis of a nonlinear mathematical model for typhoid fever disease," *Scientific Reports,* vol. 13, pp. 15284, 2023.

[26] M. Sinan, K. Shah, P. Kumam, I. Mahariq, K. J. Ansari, Z. Ahmad, and Z. Shah, "Fractional order mathematical modeling of typhoid fever disease," *Results in Physics,* vol. 32, pp. 105044, 2022.

[27] A. Elsonbaty, W. Adel, A. Aldurayhim, and A. El-Mesady, "Mathematical modeling and analysis of a novel monkeypox virus spread integrating imperfect vaccination and nonlinear incidence rates," *Ain Shams Engineering Journal,* vol. 15, pp. 102451, 2024.

[28] B. Liu, S. Farid, S. Ullah, M. Altanji, R. Nawaz, and S. W. Teklu, "Mathematical assessment of monkeypox disease with the impact of vaccination using a fractional epidemiological modeling approach," *Scientific Reports,* vol. 13, pp. 13550, 2023.

[29] M. Ngungu, E. Addai, A. Adeniji, U. M. Adam, and K. Oshinubi, "Mathematical epidemiological modeling and analysis of monkeypox dynamics with non-pharmaceutical intervention using real data from United Kingdom," *Frontiers inPublic Health,* vol. 11, pp. 1101436, 2023.

[30] P. V. D. Driessche and J. Watmough, "Reproduction numbers and sub-threshold endemic equilibria for compartmental models of disease transmission," *Mathematical bioscience,* vol. 180, pp. 29-48, 2002.